RSC New Journal of Chemistry

Supplementary Information for

A phosphorescent fluoride probe based on Eu(III)-DO3A clicked with 2,5-di(thien-2-yl)pyrrole scaffold

Memduh Bilmez[†⊥], Aysun Degirmenci[†], Melek Pamuk Algi[†,§], Fatih Algi[†,‡,*]

[†] ASUBTAM Memduh Bilmez BioNanoTech Lab., Aksaray University, TR-68100 Aksaray, Turkey.

[§] Health Services Vocational School, Aksaray University, TR-68100 Aksaray, Turkey.

[‡] Department of Biotechnology and Molecular Biology, Aksaray University, TR-68100 Aksaray, Turkey.

[⊥] Deceased

1. NMR, FTIR and MALDI-TOF-MS characterizations

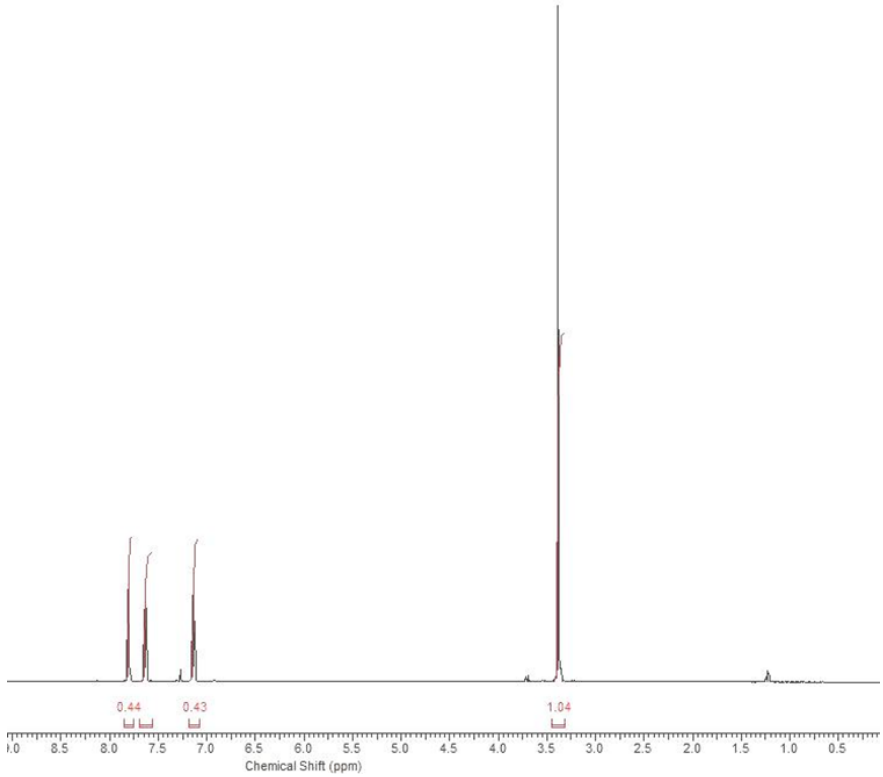

Figure S1. ^{1}H NMR spectrum of 1,4-Di(thiophen-2-yl)butane-1,4-dione **4** ($CDCl_3$).

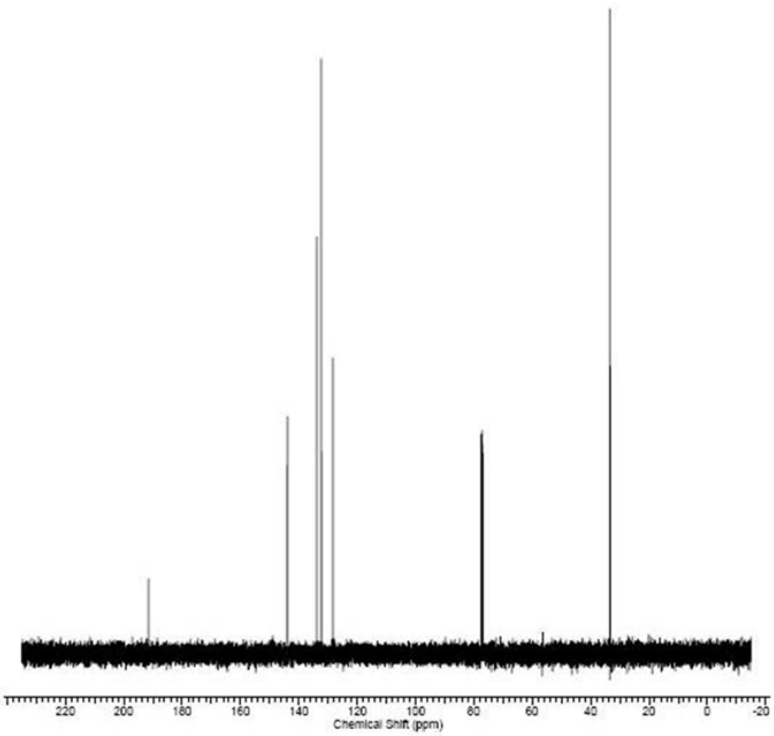

Figure S2. ^{13}C NMR spectrum of 1,4-Di(thiophen-2-yl)butane-1,4-dione **4** ($CDCl_3$).

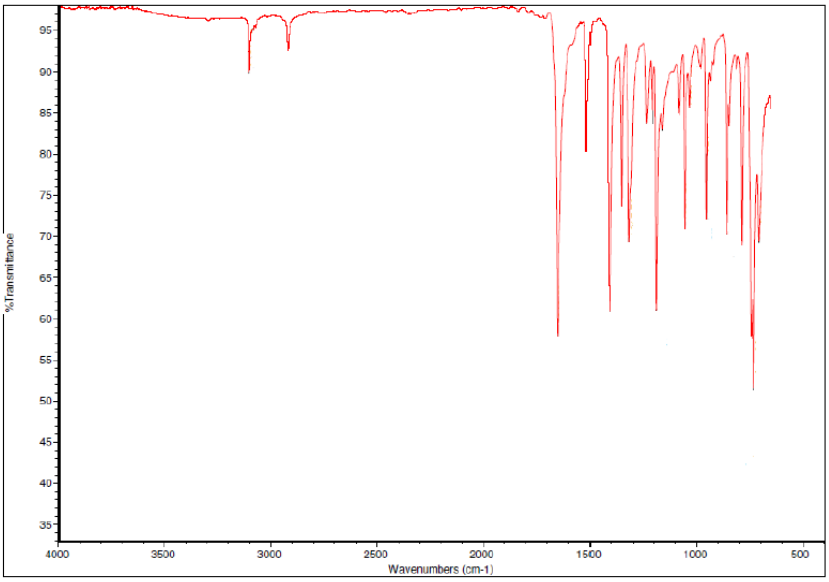

Figure S3. FTIR spectrum of 1,4-Di(thiophen-2-yl)butane-1,4-dione **4**.

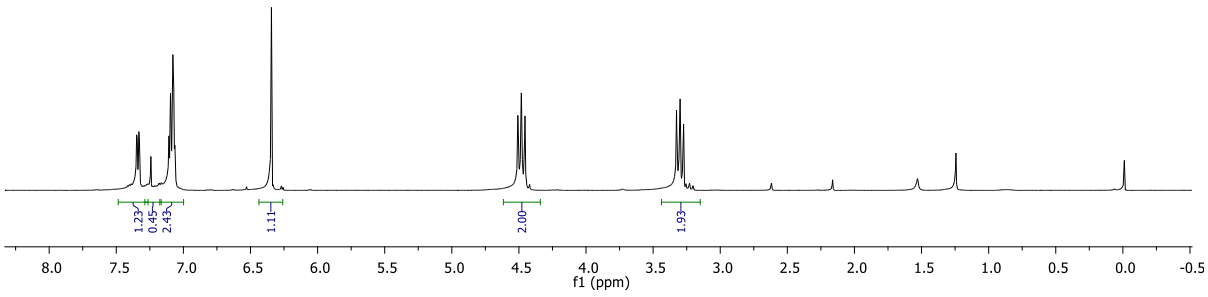

Figure S4. ^{1}H NMR spectrum of 1-(2-Bromoethyl)-2,5-di(thiophen-2-yl)-1H-pyrrole **6** ($CDCl_3$).

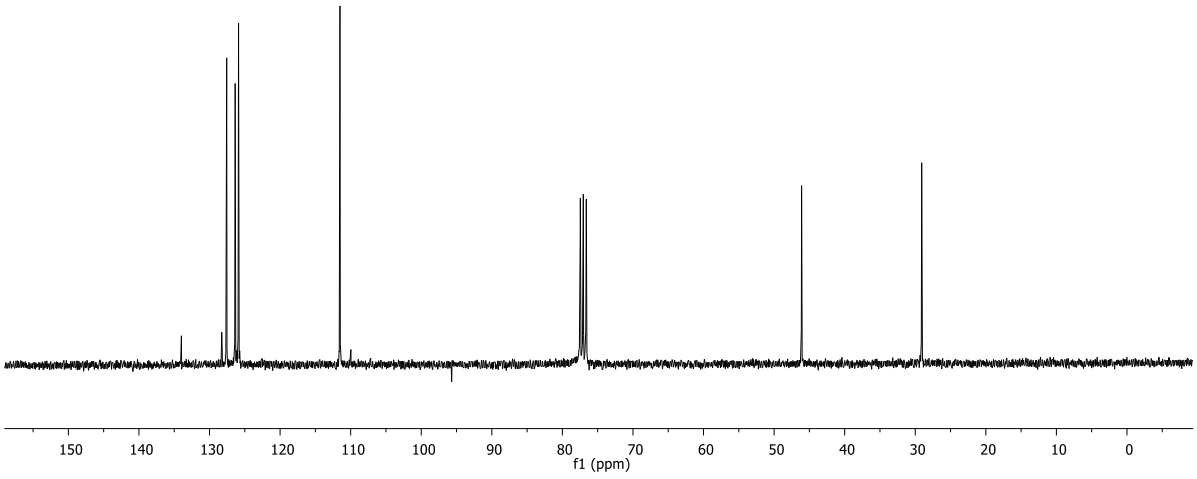

Figure S5. ^{13}C NMR spectrum of 1-(2-Bromoethyl)-2,5-di(thiophen-2-yl)-1H-pyrrole **6** ($CDCl_3$).

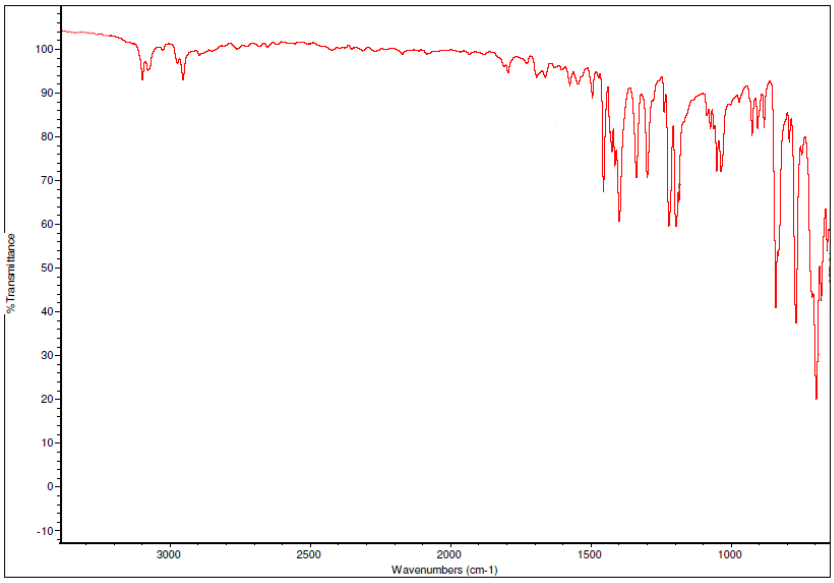

Figure S6. FTIR spectrum of 1-(2-Bromoethyl)-2,5-di(thiophen-2-yl)-1H-pyrrole **6**.

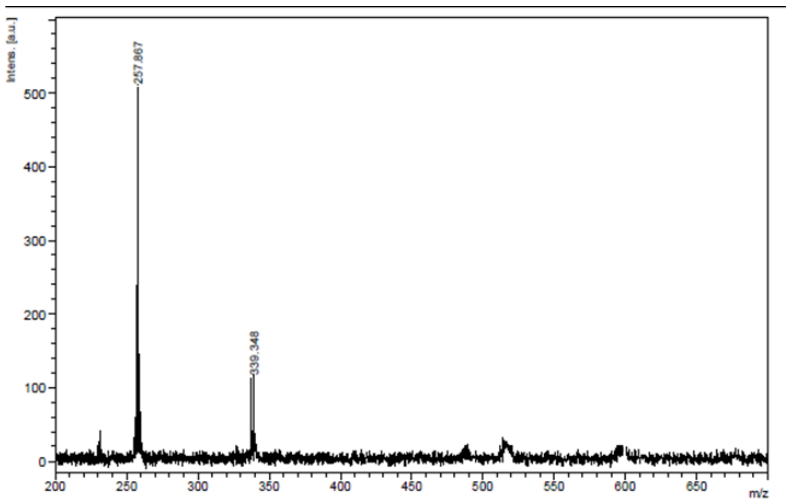

Figure S7. MALDI-TOF mass spectrum of 1-(2-Bromoethyl)-2,5-di(thiophen-2-yl)-1H-pyrrole **6**.

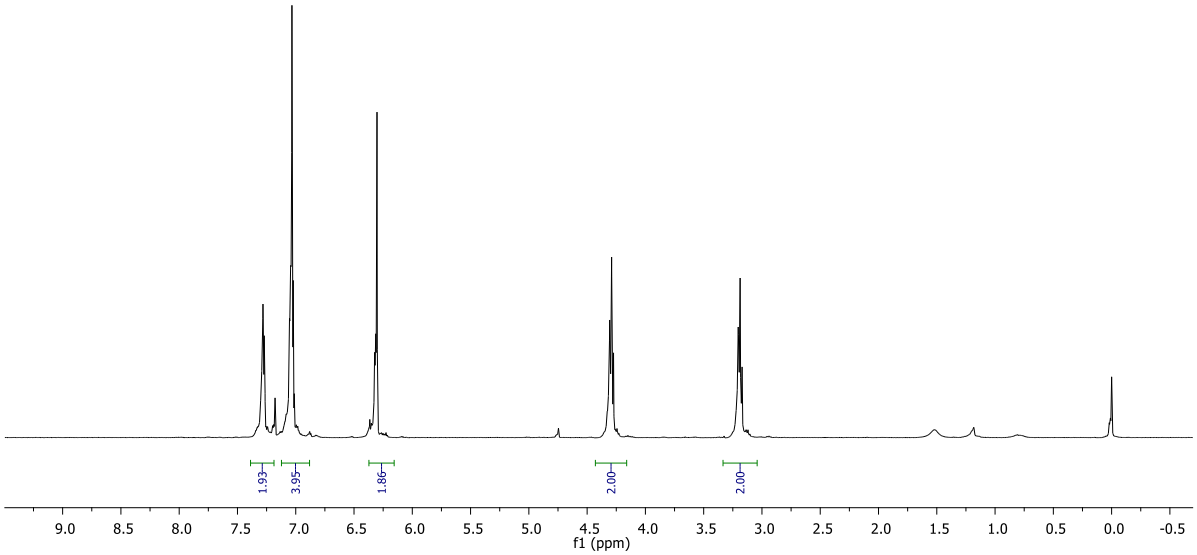

Figure S8. ^{1}H NMR spectrum of 1-(2-Azidoethyl)-2,5-di(thiophen-2-yl)-1H-pyrrole **7** ($CDCl_3$).

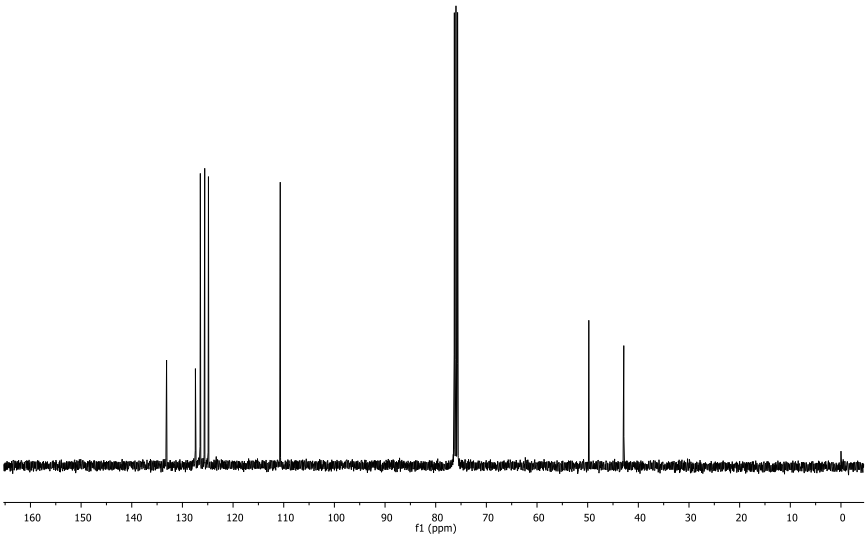

Figure S9. ^{13}C NMR spectrum of 1-(2-Azidoethyl)-2,5-di(thiophen-2-yl)-1H-pyrrole **7** ($CDCl_3$).

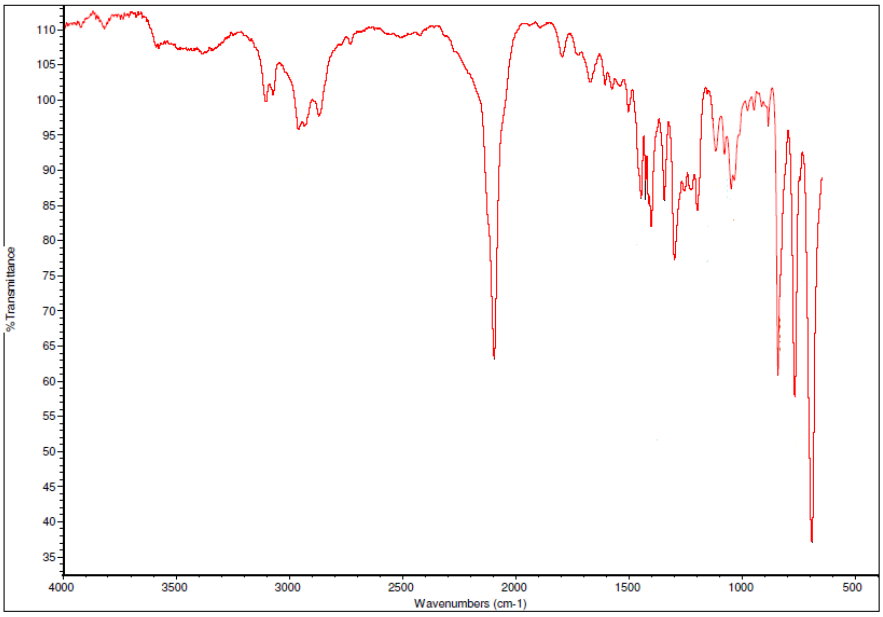

Figure S10. FTIR spectrum of 1-(2-Azidoethyl)-2,5-di(thiophen-2-yl)-1H-pyrrole **7**.

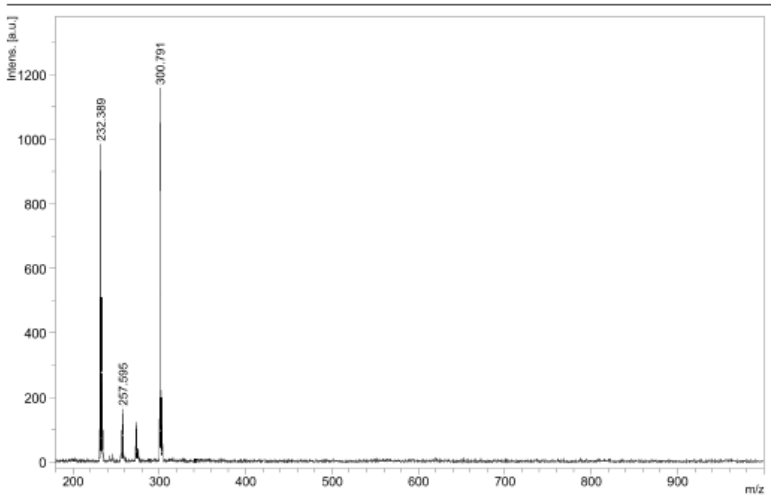

Figure S11. MALDI-TOF mass spectrum of 1-(2-Azidoethyl)-2,5-di(thiophen-2-yl)-1H-pyrrole **7**.

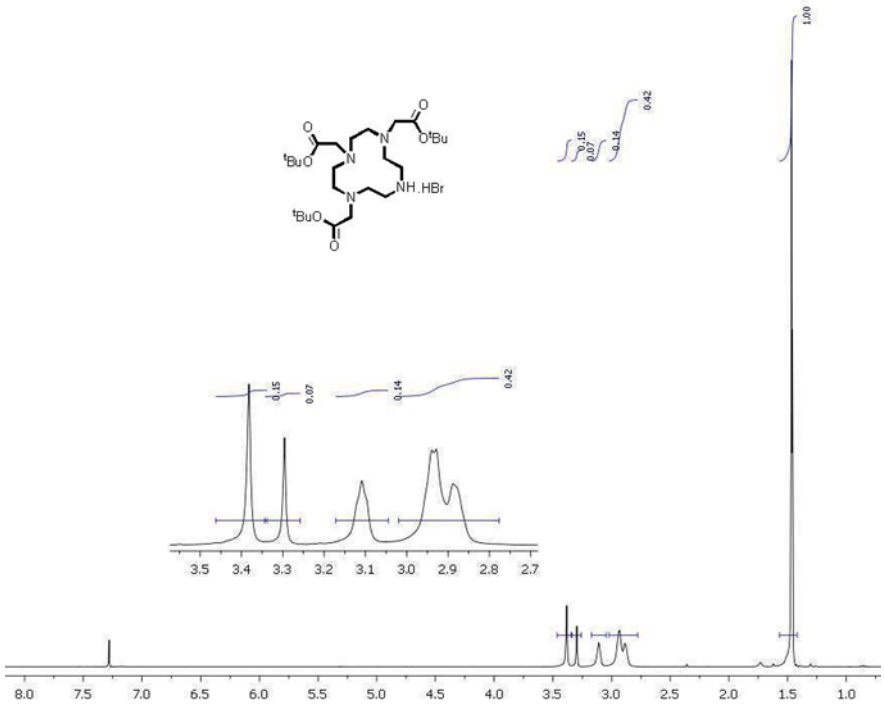

Figure S12. ^{1}H NMR spectrum of 1,4,7-tris(tert-butoxycarboxymethyl)-1,4,7,10-tetraazacyclododecane **10** ($CDCl_3$).

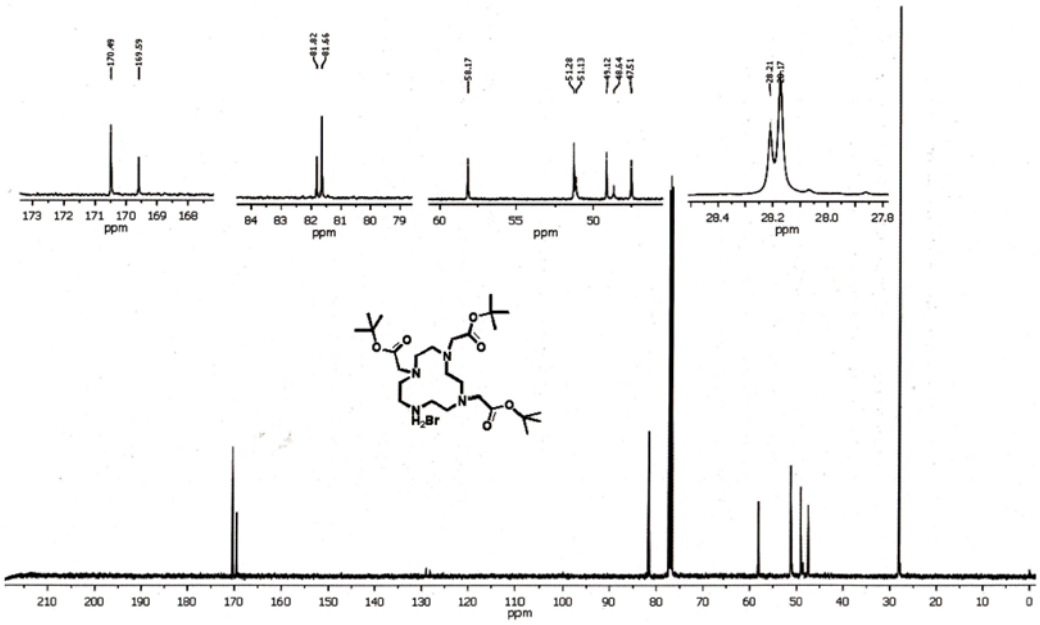

Figure S13. ^{13}C NMR spectrum of 1,4,7-tris(tert-butoxycarboxymethyl)-1,4,7,10-tetraazacyclododecane **10** ($CDCl_3$).

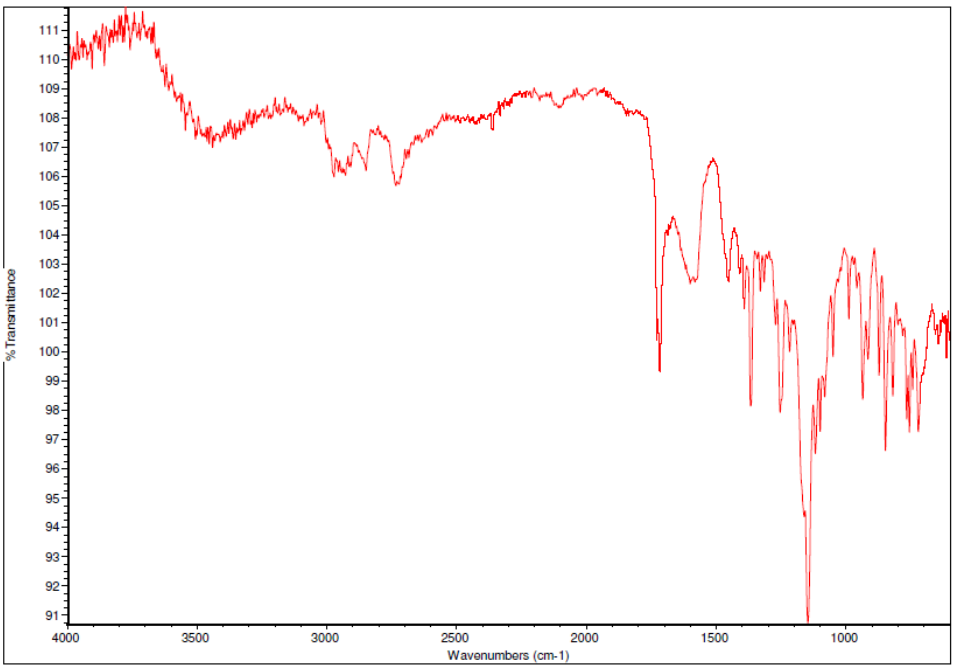

Figure S14. FTIR spectrum of 1,4,7-tris(tert-butoxycarboxymethyl)-1,4,7,10-tetraazacyclododecane **10**.

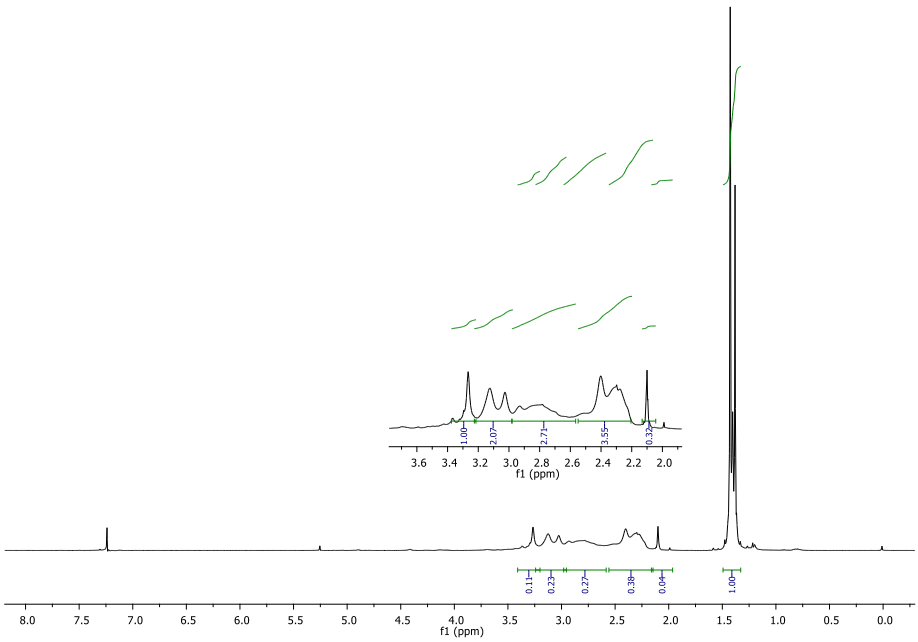

Figure S15. ^{1}H NMR spectrum of 1,4,7-tris(tert-butoxycarbonylmethyl)-10-(prop-2-yn)-1,4,7,10-tetraazacyclododecane **12** ($CDCl_3$).

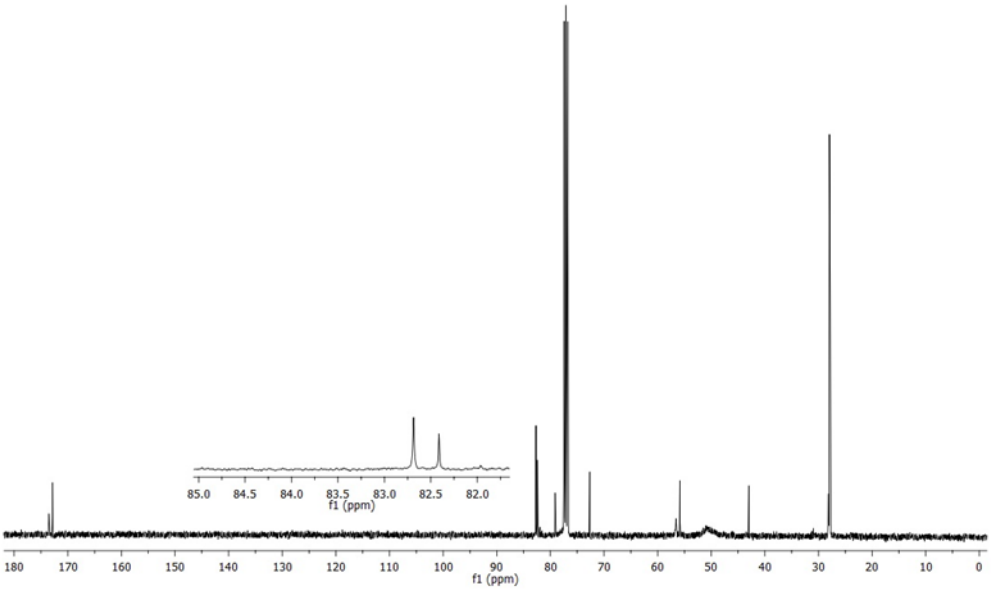

Figure S16. ^{13}C NMR spectrum of 1,4,7-tris(tert-butoxycarbonylmethyl)-10-(prop-2-yn)-1,4,7,10-tetraazacyclododecane **12** ($CDCl_3$).

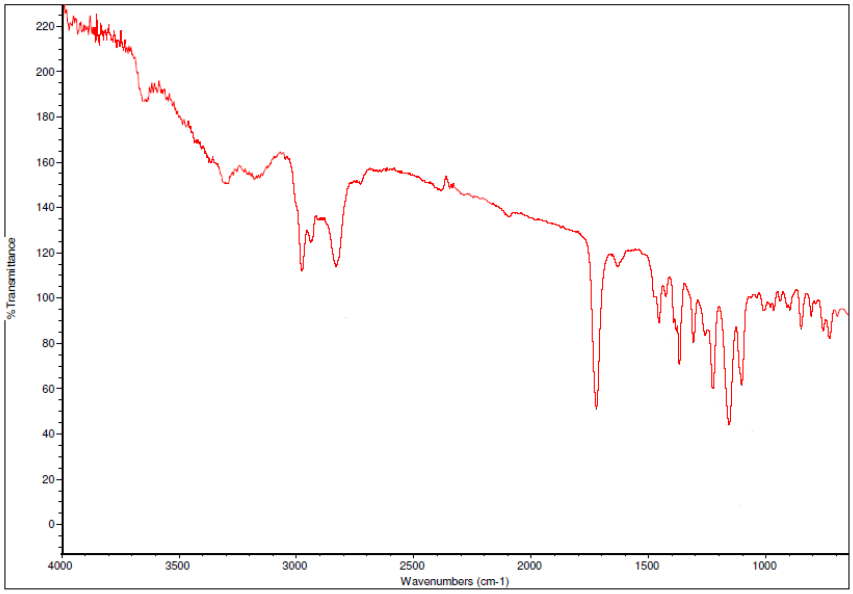

Figure S17. FTIR spectrum of 1,4,7-tris(tert-butoxycarbonylmethyl)-10-(prop-2-yn)-1,4,7,10-tetraazacyclododecane **12**.

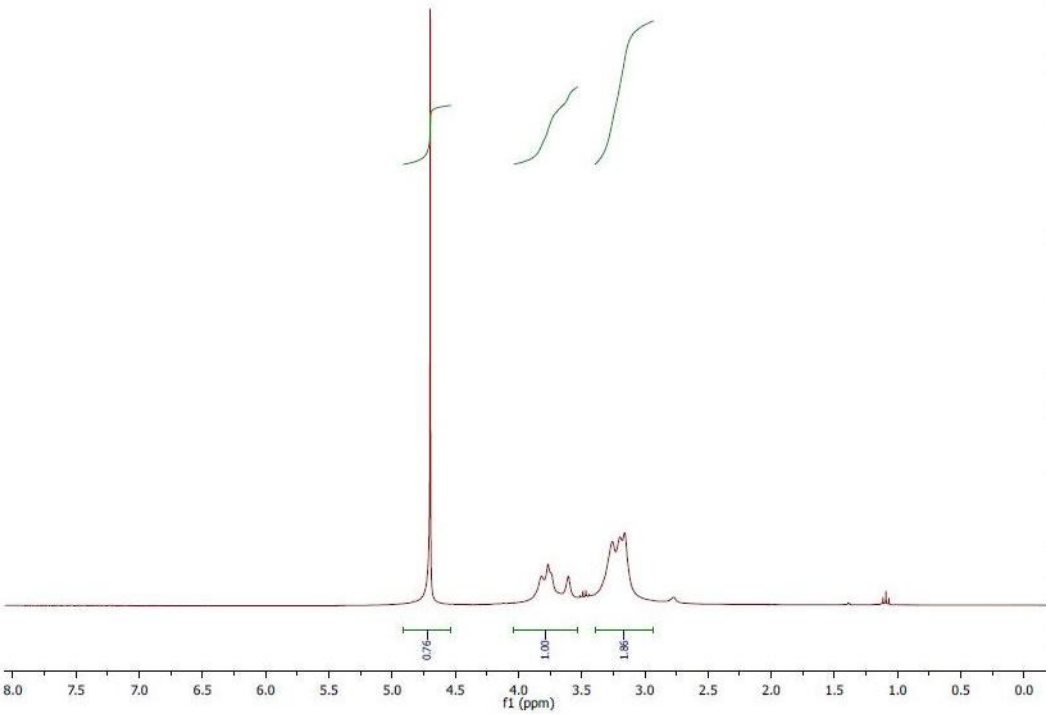

Figure S18. ^{1}H NMR spectrum of 1,4,7-tris(carboxymethyl)-10-(prop-2-ynyl)-1,4,7,10-tetraazacyclododecane **13** (D_2O).

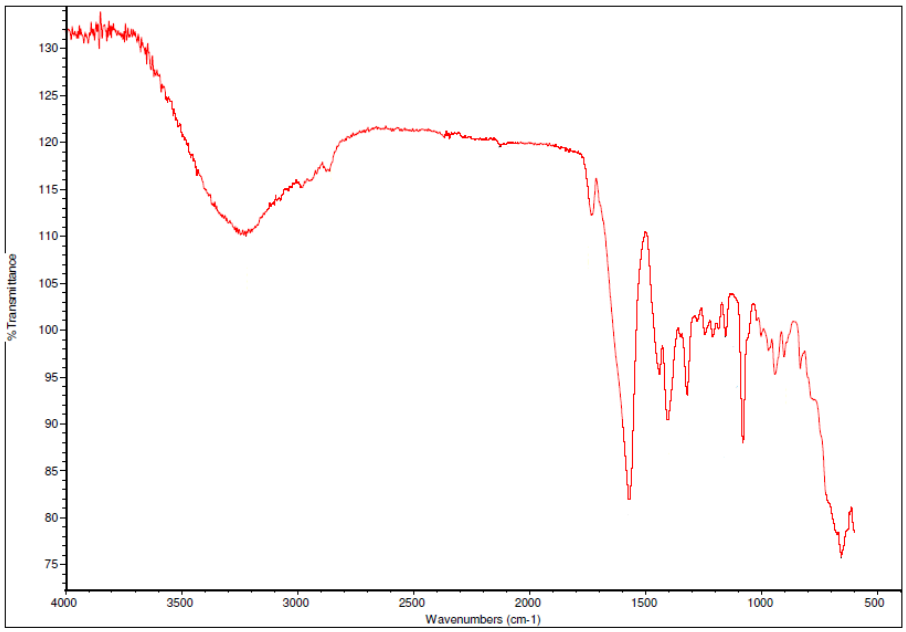

Figure S19. FTIR spectrum of 1,4,7-tris(carboxymethyl)-10-(prop-2-ynyl)-1,4,7,10-tetraazacyclododecane **13.**

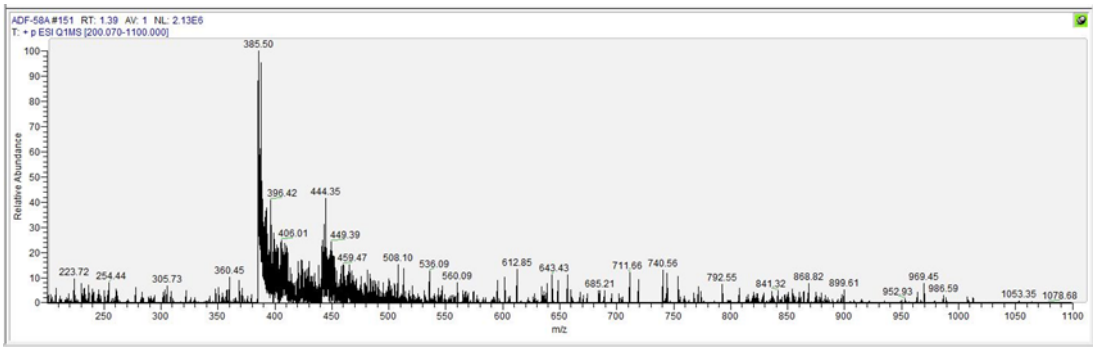

Figure S20. LC-MS spectrum of 1,4,7-tris(carboxymethyl)-10-(prop-2-ynyl)-1,4,7,10-tetraazacyclododecane **13**.

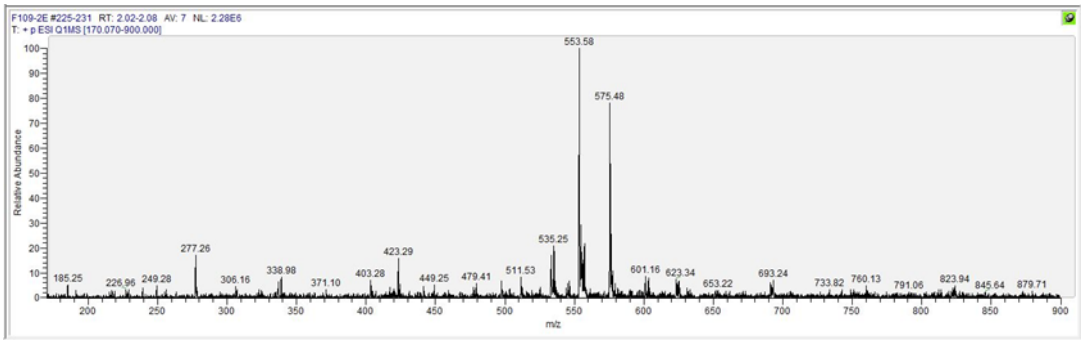

Figure S21. LC-MS spectrum of Eu complex **14**.

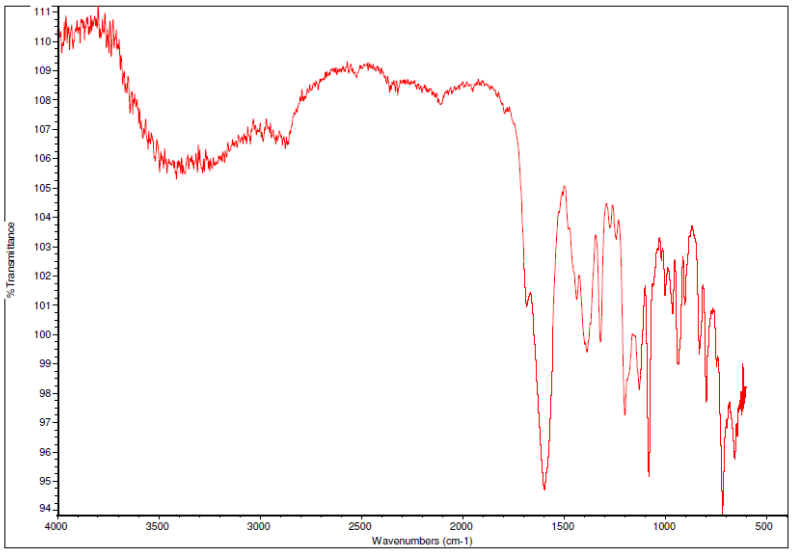

Figure S22. FTIR spectrum of Eu complex **14.**

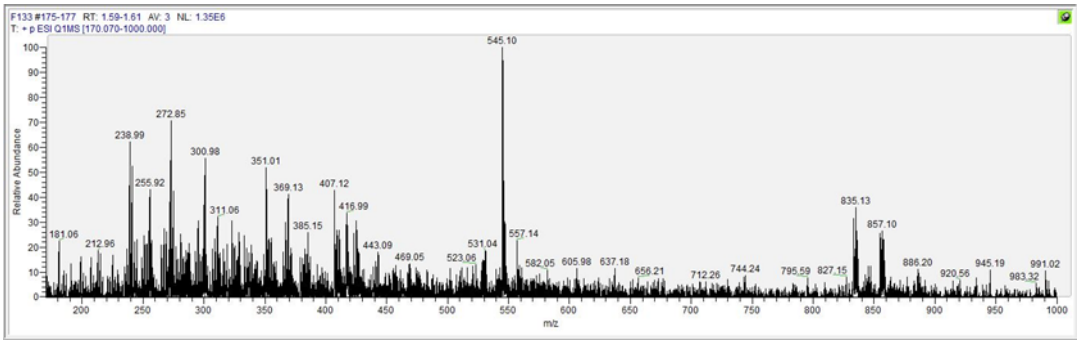

Figure S23. LC-MS spectrum of **1**.

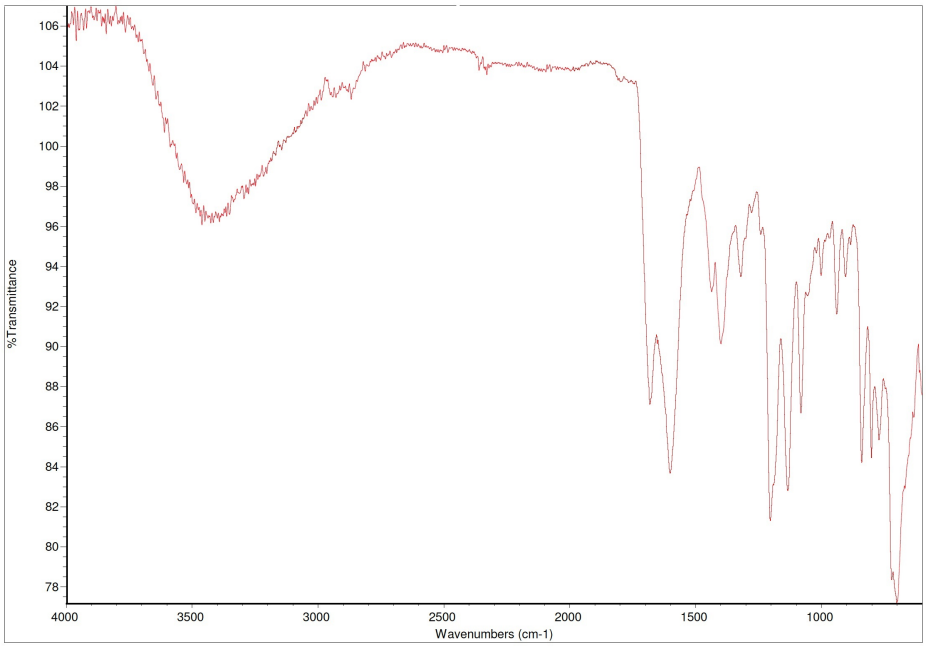

Figure S24. FTIR spectrum of **1**.

2. Additional Data

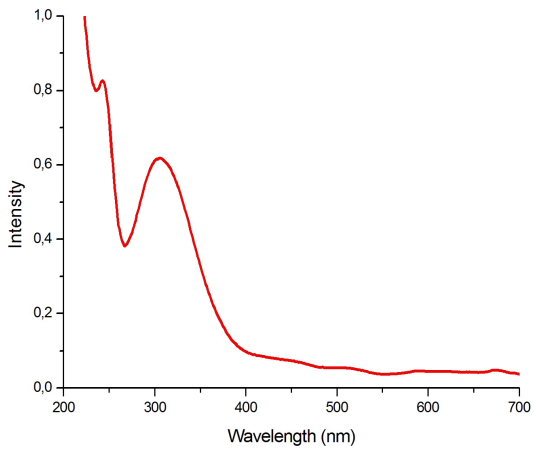

Figure S25. UV-Vis absorption spectrum of **1** (5 x 10^{-5} M) in CH_3CN.

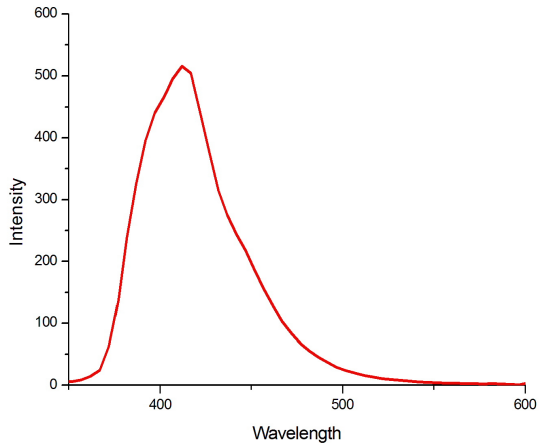

Figure S26. Fluorescence spectrum of **1** (0.8 x 10^{-5} M) in CH_3CN (λ_{exc} = 305 nm).

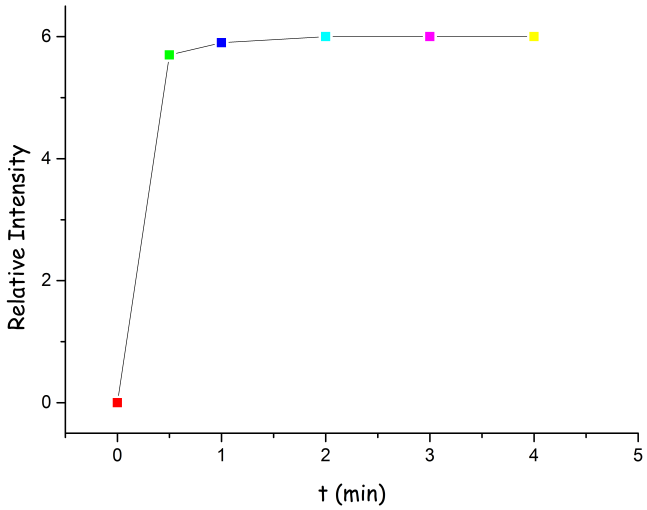

Figure S27. Response time of **1** to fluoride anion (2 equiv).

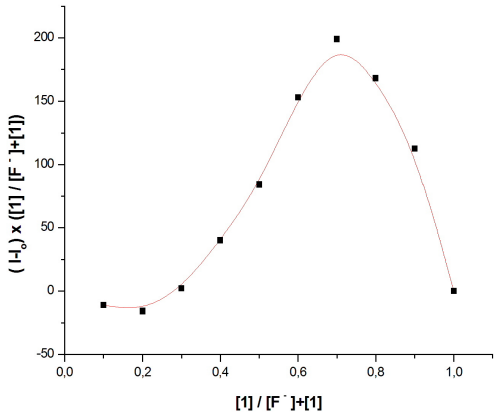

Figure S28. Job plot diagram of **1** for F^-. ($I-I_0$) indicates the change of emission intensity (@615 nm) at a constant total concentration of 8.0 μM in CH_3CN at room temperature.

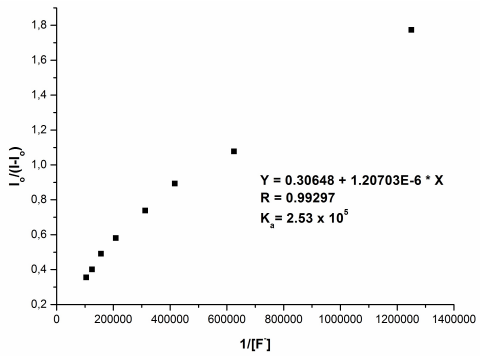

Figure S29. Linear regression curve for **1**.

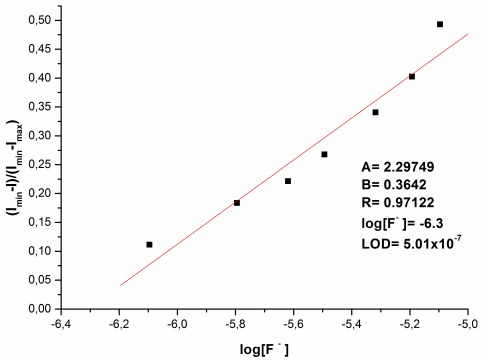

Figure S30. Plot of normalized emission intensity of **1** as a function of log[F^-] in CH_3CN at 25°C, (log[F^-] = -6.30).

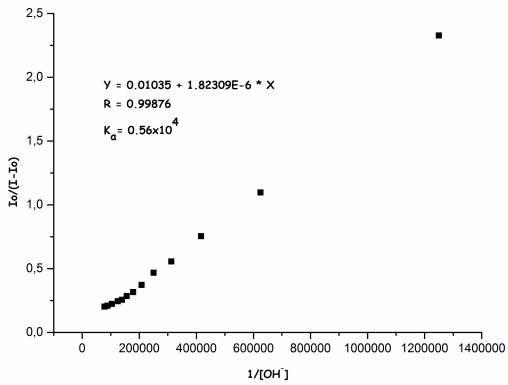

Figure S31. Linear regression curve for **1** (OH^-).

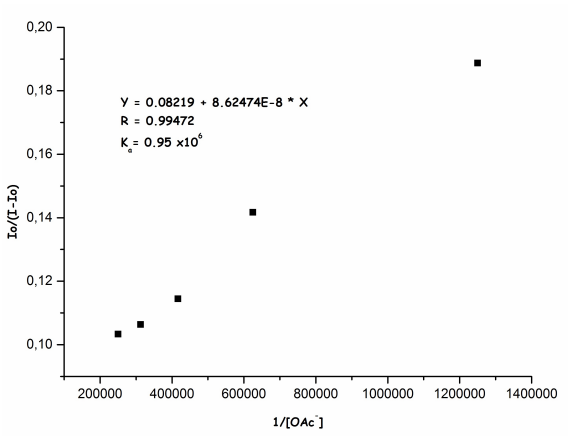

Figure S32. Linear regression curve for **1.** (AcO^-)

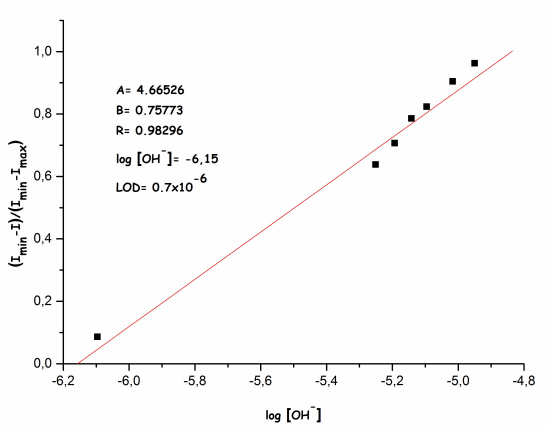

Figure S33. Plot of normalized emission intensity of **1** as a function of log[OH^-] in CH_3CN at 25°C, (log[OH^-] = -6.15).

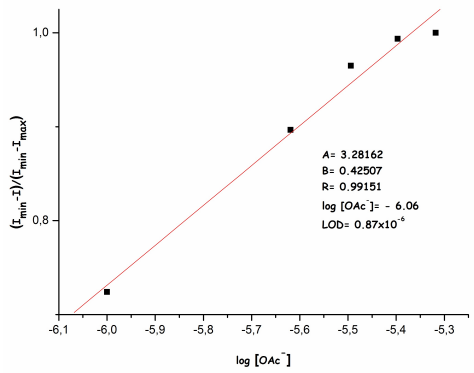

Figure S34. Plot of normalized emission intensity of **1** as a function of log[OAc^-] in CH_3CN at 25°C, (log[OAc^-] = -6.06).